Journal of Electronic Materials (2021) 50:4908–4914
https://doi.org/10.1007/s11664-021-09018-z

ORIGINAL RESEARCH ARTICLE

Improving the Thermal Stability and Oxidation Resistance of Silver Nanowire Films via 2-Mercaptobenzimidazole Modification

Junfei Ma[1,2] · Ji-Hyeon Kim[1] · Ga Hyun Lee[1,2] · Sungjin Jo[2] · Chang Su Kim[1]

Received: 5 January 2021 / Accepted: 14 May 2021 / Published online: 7 June 2021

Abstract

For electronic devices, a tradeoff exists between the structural stability and electrical conductivity of silver nanowires (Ag NWs). Self-assembled monolayers (SAMs) containing sulfur functional groups formed on the Ag nanowire surface through Ag–S covalent bonds can act as a passivation layer, thereby improving the corrosion resistance. This work explored the effect of 2-mercaptobenzimidazole (MBI) SAM on the thermal and oxidation resistance of Ag NW films. The conductivity, surface morphology, chemical properties, and thermal stability of MBI-modified Ag NW films were analyzed via four-point probe measurements, field-emission scanning electron microscopy, x-ray photoelectron spectroscopy (XPS), and thermal characterization. In particular, the results show that the MBI layer can significantly reduce the oxidation of Ag NW films at room temperature for 60 days. Moreover, the MBI layer improved the thermal stability of the Ag NW films up to 230°C by inhibiting Ag diffusion. The unmodified Ag NW film completely lost conductivity after heating and oxidation treatment. In contrast, the sheet resistance of the Ag NW film modified by 0.1 wt.% MBI only increased from 65 Ω/□ to 106 Ω/□, and 156 Ω/□ after heating treatment and oxidation test, respectively.

Keywords Silver nanowire · 2-mercaptobenzimidazole · oxidation resistance · transparent conductive film · thermal stability · self-assembled monolayers

Introduction

In the last few decades, indium tin oxide (ITO) has been widely used as a transparent electrode material due to its low sheet resistance and visible light transmission of approximately 90% at a wavelength of 420 nm.[1] However, the brittle ITO layer can be easily cracked and damaged by external forces, making it no longer suitable for next-generation flexible electronic devices, including wearable devices, slim flexible displays, resistance switching memory,[2,3] and mobile phones.[4] Therefore, developing new materials to replace ITO for flexible transparent electrodes has become a widely researched topic. Many potentially valuable materials can replace ITO in solar cells and organic light-emitting diodes (OLED). These include carbon nanotubes (CNTs),[5-7] aluminum-doped zinc oxide (AZO),[8,9] fluorine-doped tin oxide (FTO),[10] indium gallium zinc oxide (IGZO),[11] metal meshes,[12,13]graphene,[14,15] poly(3,4-ethylene dioxythiophene):poly (styrene sulfonate) (PEDOT:PSS),[16-18] and Ag nanowires (NWs).[19,20] However, these materials have a variety of disadvantages. The worse continuity of nanotubes compared with ITO may affect the electrical conductivity of carbon nanotubes.[21] The low availability of FTO and AZO leads to high prices for these materials.[22] Because IGZO contains rare metals (indium and gallium), its processing cost is high. Compared with ITO, metal grids suffer from poor deposition.[23] Graphene's complex processing technology limits large-area production.[24] To increase the conductivity, the

✉ Sungjin Jo
sungjin@knu.ac.kr

✉ Chang Su Kim
cskim1025@kims.re.kr

Junfei Ma
ready@kims.re.kr

Ji-Hyeon Kim
sangdu87@kims.re.kr

Ga Hyun Lee
gaataan2@kims.re.kr

[1] Department of Nano-Bio Convergence, Korea Institute of Materials Science (KIMS), 797 Changwondaero, Seongsan-gu, Changwon 51508, South Korea

[2] School of Architectural, Civil, Environmental, and Energy Engineering, Kyungpook National University, 80 Daehakro, Bukgu, Daegu 41566, South Korea

PODET:PSS surface treated with strong acid may produce a certain degree of corrosion on flexible Ag NW substrates.[25] Consequently, considering the production cost, optical performance, electrical conductivity, mechanical properties, and other factors, Ag NWs are considered to be the most promising material as an alternative to ITO.[26,27] However, in the absence of the passivation layer, the main disadvantages of Ag NWs include oxidation and thermal instability when exposed to air or a continuously passing current.[28,29] These disadvantages prevent the application of these nanowires in transparent conductive devices. To improve the oxidation resistance and thermal stability of Ag NW films in air or other special environments, many scientists have combined Ag NWs with other materials or surface-modified Ag NWs; For example, graphene oxide or graphene/Ag NW,[30,31] PEDOT:PSS/Ag NW/graphene oxide,[32] zinc oxide/Ag NW,[33] laser-reduced Ag NW,[34] acrylate/Ag NW,[35] electron-beam-irradiated Ag NW,[36] and Ag–Au nanocomposite have been investigated.[37] Most researches have aimed to improve the structural-level connections between Ag NWs and nanomaterials. These strategies include increasing the number of layers and thickness of the composite film, thus improving the oxidation resistance while reducing optical transparency. Therefore, identifying a functional material that improves the thermal stability and oxidation resistance of Ag NW films without compromising their excellent optical transmission properties is of utmost importance.

2-Mercaptobenzimidazole (MBI) has garnered significant attention as an anticorrosion layer due to its ability to block the migration and contact of metal atoms with oxygen, thereby maintaining the excellent conductivity of metallic materials in harsh environments.[38-41] To the best of the authors' knowledge, there are some articles on the study of MBI molecules as a self-assembled layer to maintain the high-temperature resistance of Ag NW. In this work, by immersing the Ag NWs film in transparent MBI ethanol solution, a self-assembled MBI molecular layers was formed on the surface of Ag NWs. We explored the effect of using different concentrations of MBI solution on the Ag NWs and determined the best MBI solution concentration to improve the thermal and oxidation resistance of the Ag NW film. Moreover, the results of the thermal and oxidation resistance experiments reval that MBI can not only prevent Ag NWs from melting at 230°C for up to 1 h, but also effectively protect the Ag NWs from oxidation in air for up to 60 days.

Experimental Procedures

Materials

This study utilized Ag NWs with average length of 20 μm and diameter of 20 nm. The Ag NWs were dispersed in isopropyl alcohol (IPA) to make 0.3 wt.% Ag NW ink. Ag NW ink with a polyvinylpyrrolidone (PVP) capping layer was purchased from C3Nano Co., Ltd. (Hayward, USA). 2-Mercaptobenzimidazole powder was obtained from Sigma Aldrich Co., Ltd. (St. Louis, USA)

Preparation of MBI/Ag NW Films

Initially, 0.02 g or 0.06 g MBI powder was weighed using an ML-T analytical balance (ML204T/00, Mettler Toledo, USA), then dissolved in 20 g ethanol with purity of 99.9%. The mixture was sonicated (SD 200H, Wan Kyung Tech, Korea) for 10 min to accelerate dissolution of MBI in ethanol and obtain uniform and colorless 0.1 wt.% and 0.3 wt.% MBI solutions. Glass substrates were cleaned by sonication with acetone and IPA for 10 min each. Then, the cleaned glass substrates were dried in a drying cabinet at 100°C for 10 min to evaporate any remaining organic matter. The 0.3 wt.% Ag NW suspension solution was deposited on the clean glass by spin coating (ACE-200, Dong Ah Trade Corp, Korea) at 3000 rpm for 30 s. Subsequently, the Ag NW film on glass was dried on a hot plate at 120°C for 1 min to evaporate the organic molecules and form a more stable two-dimensional network by promoting the welding of Ag NW to each other. As seen in Fig. 1a, the MBI layer was formed on Ag NWs via a sol–gel system. The heated Ag NW films were immersed in the previously prepared MBI ethanol solutions for 30 min, being denoted as 0.1 wt.% MBI/Ag NW and 0.3 wt.% MIB/Ag NW, respectively. The MBI and Ag NW composite films were dried at room temperature for 10 min to remove the remaining ethanol and form the MBI layer by evaporation naturally.

Results and Discussion

UV–Vis Spectroscopy Analysis

The transmittance characteristics of the films as measured using an ultraviolet–visible–near infrared (UV–Vis–NIR) spectrophotometer (Carry 5000, Agilent, USA) are shown in Fig. 1b. The transmittance of Ag NW, 0.1 wt.% MBI/Ag NW, and 0.3 wt.% MBI/Ag NW is marked as T_A, $T_{0.1}$, and $T_{0.3}$, respectively. The transmittances of the three samples lies in the order: $T_A > T_{0.1} > T_{0.3}$. The transmittance of the MBI/Ag NW films decreased as the MBI flakes generated a self-assembled layer adsorbed on the surface of the Ag NWs.[42] However, the transmittance of the 0.1 wt.% MBI/Ag NW film and 0.3 wt.% MBI/Ag NW samples was 85.0% and 80.0% at a wavelength of 500 nm, respectively. Notably, we confirmed that increasing the thickness of the MBI molecular layer had a negative influence on the light transmittance of the Ag NW film and that the optical transparency of the

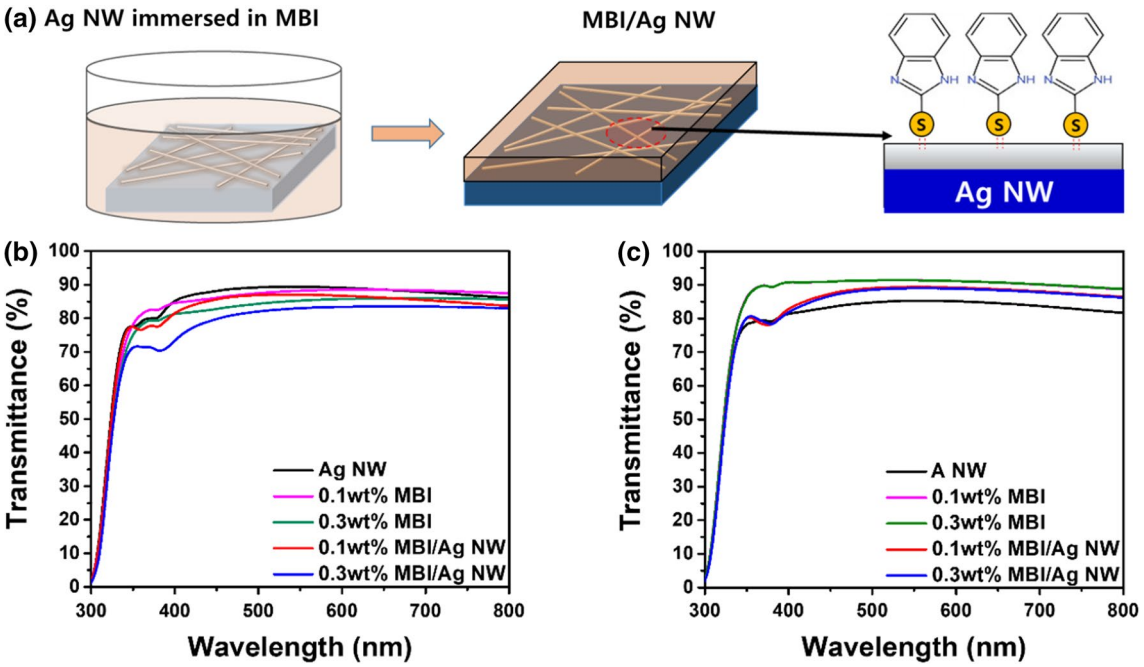

Fig. 1 (a) Schematic of process for covering glass substrates coated with Ag NW film with MBI by the immersion method. Transmittance spectra of MBI film, pristine Ag NW film, and MBI-decorated Ag NW composite film (b) before and (c) after drying at 230°C for 1 h

MBI-functionalized Ag NWs also depended on the concentration of the MBI. The transmittance after drying is shown in Fig. 1c, showing that the transmittance of the three films lies in the order: $T_{0.1} > T_{0.3} > T_A$. The main reason for the change is that the Ag NWs were fused by heat to form silver nanoparticles (Ag NPs) with larger diameters, increasing the surface roughness and the light absorption rate of the Ag NW and thereby reducing the transmittance of the Ag NW film.[43] On the other hand, the 0.1 wt.% MBI layer produced volatilization after heating, which increased the transmittance of the MBI/Ag NW film. In the 0.3 wt.% MBI/Ag NW film, although most of the MBI layer was volatilized after heating, the transmittance increased but many silver oxide nanoparticles were produced on the surface of the Ag NWs, resulting in a transmittance slightly lower than that of the 0.1 wt.% MBI/Ag NW film.

SEM and XPS Analyses

The structural morphology of the Ag NW, 0.1 wt.% MBI/Ag NW, and 0.3 wt.% MBI/Ag NW without heat treatment is illustrated in Fig. 2a, b, and c, respectively. The transmittance of the 0.1 wt.% MBI-coated Ag NW film was not significantly lower than that of the pristine Ag NW film. The MBI molecules did not affect the transmittance of the Ag NW film because the low concentration of the MBI solution was not sufficient to form a complete layer adsorbed on the Ag NW film. Conversely, the transmittance of the Ag NW film soaked in 0.3 wt.% MBI solution was significantly reduced because the Ag NW was distributed under a thicker MBI layer. Besides, there were many structural defects in the 0.3 wt.% MBI film, which weakened the inhibition of the diffusion of Ag atoms when heated. Figure 2d, e, and f show the nanostructural changes in the Ag NW film, 0.1 wt.% MBI/Ag NW film, and 0.3 wt.% MBI/Ag NW film, respectively, after heat treatment for 60 min, exhibiting the fusion of Ag NWs by heat to form smaller nanoparticles and nanorods. The phenomenon of Ag NWs fusing into silver nanoparticles at high temperatures is due to the Rayleigh instability of metals.[44,45] However, the 0.1 wt.% MBI/Ag NW did not fuse and there were no large amounts of silver oxide particles on the surface of the Ag NWs (Fig. 2e). Due to the thiol functional groups forming more stable Ag–S bonds with Ag atoms, MBI was volatilized and a thinned out-layer composed of S–Ag bonds with a higher melting point than Ag–Ag bonds was left, preventing the diffusion of atoms on the surface of the Ag NWs after heating.[46] Compared with the Ag NW film, although the 0.3 wt.% MBI layer protected the Ag NW film from fusing after heating at 230°C (Fig. 2f), a large number of nanoparticles were attached to the Ag NWs because of defects in the MBI layer before heating. As illustrated in Fig. 2g, the sheet resistance of the 0.1 wt.% MBI/Ag NW sample indicated better thermal resistance. The sheet resistance of the pristine Ag NW film was measured to be 57 Ω/□

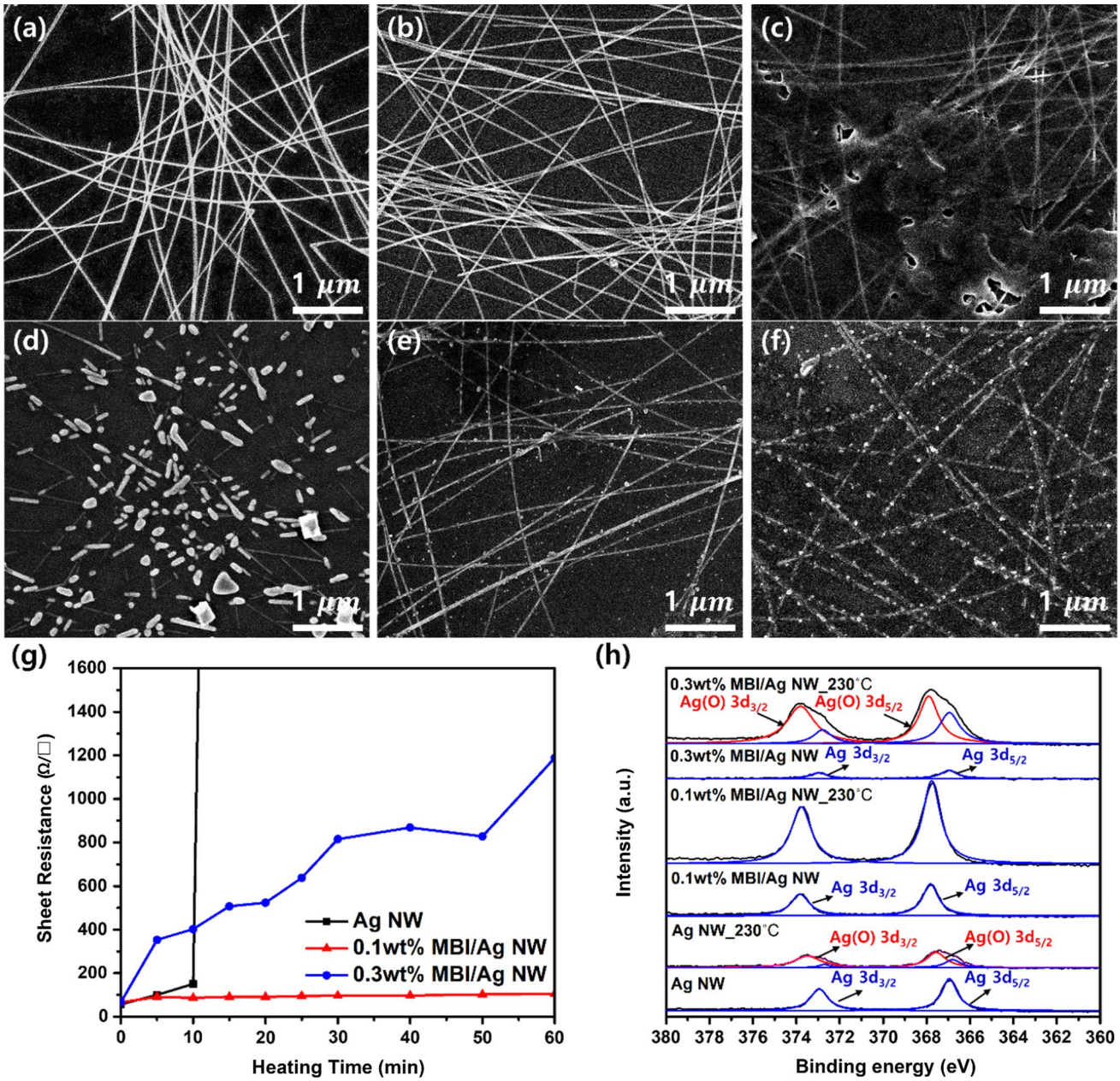

Fig. 2 Morphologies of (a, d) Ag NW, (b, e) 0.1 wt.% MBI/Ag NW, (c, f) 0.3 wt.% MBI/Ag NW samples observed before and after heat treatment at 230°C for 60 min, respectively. (g) The resistance curve of Ag NW, 0.1 wt.%, and 0.3 wt.% MBI/Ag NW films after heating at 230°C for 60 min. (h) Ag 3*d* core-level XPS spectra of Ag NW, 0.1 wt.% MBI/Ag NW, and 0.3 wt.% MBI/Ag NW before and after heating at 230°C for 60 min

in the initial state. The sheet resistance of the Ag NW film immersed in the 0.1 wt.% MBI solution was 65 Ω/□. The sheet resistance of the MBI/Ag NW film increased slightly because of the MBI layer adsorbed on the AgNW structures. When heated to 230°C, the sheet resistance of the Ag NW film without MBI increased quickly and completely lost conductivity after a heating time of only 10 min compared with the 0.3 wt.% MBI/Ag NW. The resistance of the 0.3 wt.% MBI/Ag NW sample rose from 65 Ω/□ to more than 1200 Ω/□. The sheet resistance of the 0.1 wt.% MBI/Ag NW only increased to 106 Ω/□ after a heating time of 60 min.

Figure 2h shows the Ag 3*d* XPS spectra of the three films before and after heating. In the high-resolution XPS spectra, the Ag peak of the 0.1 wt.% MBI/Ag NW film splits into a doublet with Ag $3d_{5/2}$ and Ag $3d_{3/2}$ components located at 367.8 eV and 373.8 eV, respectively.[47,48] The Ag $3d_{5/2}$ and Ag $3d_{3/2}$ bonds of the 0.1 wt.% MBI/Ag NW film also did

not shift after heating. However, the coexistence of Ag $3d_{5/2}$ and Ag $3d_{3/2}$ in Ag NW and 0.3 wt.% MBI/Ag NW before annealing is evidenced by a shoulder observed at 367.0 eV and 373.0 eV, respectively. As Ag atoms reacted with oxygen to form silver oxide nanoparticles, the binding energy of Ag atoms shifted to a higher position in the oxidized silver, marked as Ag(O) $3d_{5/2}$ (367.8 eV) and Ag(O) $3d_{3/2}$ (373.8 eV) after heating at 230°C, respectively.[49,50] These results confirmed that the 0.1 wt.% MBI layer has excellent anti-oxidation performance and effectively protects the Ag NW.

Oxidation Resistance Test

The effect of MBI concentration on the oxidation resistance of Ag NW films was investigated and the resulting sheet resistance curves are depicted in Fig. 3a. The sheet resistance of the Ag NW film increased from 57 Ω/□ to more than 10000 Ω/□ after 60 days. The sheet resistance of the 0.3 wt.% MBI/Ag NW composite film increased from 67 Ω/□ to 600 Ω/□, which is significantly lower than the growth trend of the bare Ag NW. Interestingly, as shown in blue, the sheet resistance of the 0.1 wt.% MBI/Ag NW film increased from 65 Ω/□ to 156 Ω/□. To more intuitively demonstrate the MBI-enhanced oxidation resistance of Ag NW, the three films were imaged using an SEM as can be seen from Fig. 3b, c, and d. The SEM images suggest that several silver oxide nanoparticles were formed on the surface of the Ag NWs over the 60 days. The Ag NW without an MBI passivation layer easily reacted with oxygen in the air to form numerous non-conductive silver oxide nanoparticles distributed on the surface of the Ag NW. Compared to bare Ag NW, large MBI fragments were observed on top of the 0.3 wt.% MBI/Ag NW film and small amounts of nanoparticles were also formed around them. Due to the structural defects in the 0.3 wt.% MBI layer, the Ag NW came in contact with air, which in turn led to the oxidation of the Ag NW. Conversely, the 0.1 wt.% MBI/Ag NW film surface did not have nanoparticles or large MBI fragments as the 0.1 wt.% MBI solution formed a dense monolayer coating on the Ag NW. Therefore, through SEM image analysis, we can speculate that a 0.1 wt.% MBI solution can form a protective layer on the Ag NW through Ag-S bonds and ensure that the Ag NW has great electrical conductivity and enhanced oxidation resistance.

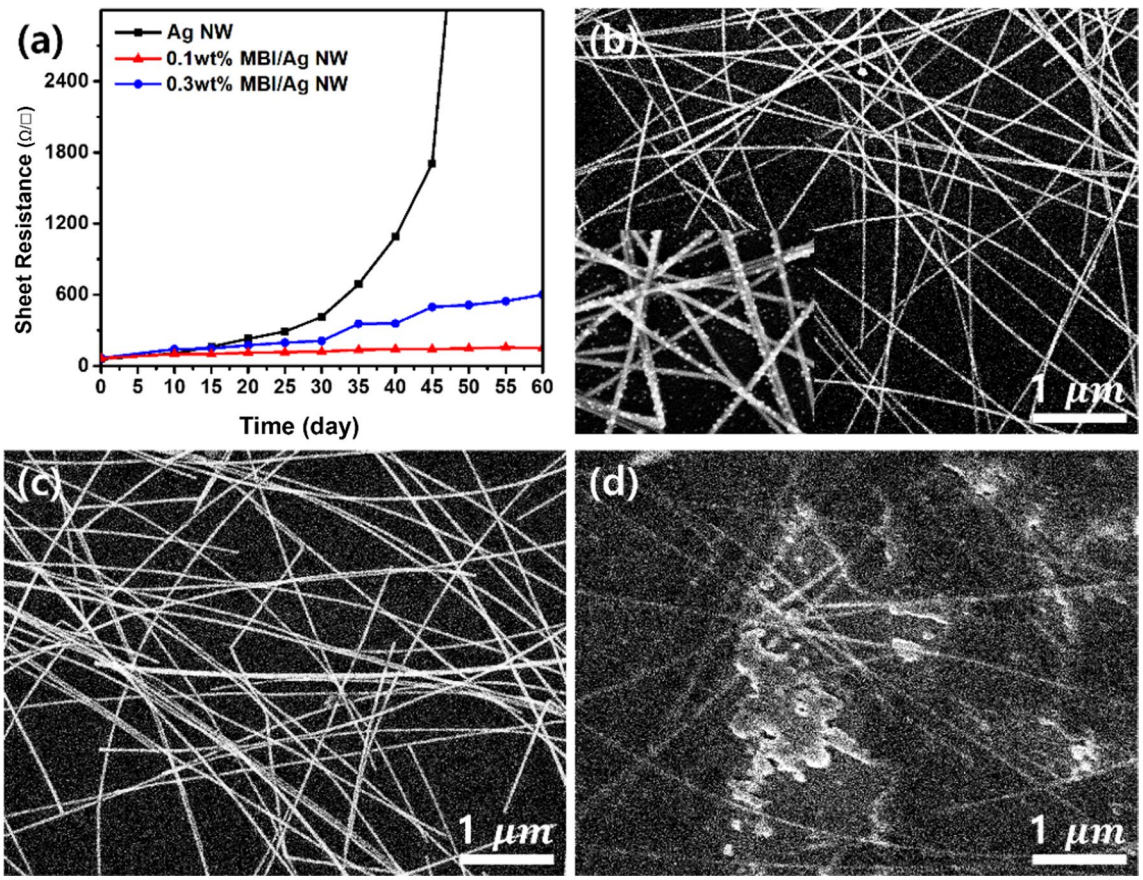

Fig. 3 (a) Sheet resistance curves of Ag NW and MBI-decorated Ag NW films stored at room temperature for 60 days. SEM images of (b) Ag NW, (c) 0.1 wt.% MBI/Ag NW, and (d) NW 0.3 wt.% MBI/Ag NW after 60 days

Compared with results previously reported in literature, this study demonstrates that the MBI layer led to improvements in the oxidation and thermal resistance of the Ag NW film. The MBI layer containing thiol groups evenly coated the surface of the Ag NWs and inhibited the diffusion of Ag atoms from the surface after it was heated at 230°C for 60 min. Conversely, replacing the MBI with 1-octanedanethiol (ODT) (St. Louis, Sigma Aldrich Co., Ltd., USA), which also contains thiol groups, and heating under the same aforementioned conditions causes the Ag NW to fuse into the Ag NPs. This is because the ODT is nonuniformly distributed on the surface of the Ag NWs, which promotes the surface diffusion of Ag atoms.[38] Therefore, the protective effect of Ag–S bonds on Ag NWs also depends on the type of thiol-containing organic compound used.

Conclusions

Thermal and oxidation resistance experiments revealed that the conductivity of 0.1 wt.% MBI/Ag NW film could be maintained at the initial level. The optical properties, chemical stability, and thermal resistance of the 0.1 wt.% MBI/Ag NW film were significantly better than those of bare Ag NW film without MBI. The initial resistance of 0.1 wt.% MBI/Ag NWs was 65 Ω/□. Although the resistance increased to 156 Ω/□ and 105 Ω/□ after oxidation and high-temperature resistance testing, respectively, it remained significantly better than the values for the 0.3 wt.% MBI/Ag NW (602 Ω/□ and 1189 Ω/□) and Ag NW (infinity and infinity) samples. Stable covalent Ag–S bonds formed between the Ag NWs and thiol groups, enabling self-assembly of the MBI monolayer to act as a passivation layer and prevent oxygen from reacting with the Ag NW. Moreover, the MBI layer on the Ag NW film can prevent the Ag NWs from melting and diffusing at high temperature. These experimental results support our view that MBI provides a unique protective mechanism for Ag NWs, thereby enabling its use for durable and thermally resistant conductive layers for solar panels, OLEDs, resistance-switching memory, transparent films, and flexible electronic devices.

Authors Contributions This experimental framework was designed and directed by C.S.K. J.M. was responsible for the progress of this experiment and analysis of the data and details with C.S.K., S.J., and J.K. J.K. contributed to contact the SEM and XPS. Lee assisted in the design and operation of this experiment. Writing—original draft preparation, J.M. writing—review and editing, J.M, J.K., S.J., and C.S.K.

Funding This research was supported by the fundamental research program (PNK7400) of the Korea Institute of Materials Science (KIMS). This research was also supported by the Technology Development Program (S2830309) funded by the Ministry of SMEs and Startups (MSS, Korea), "Nano Product Upgrading Program using Electron Beam" through the Gyeongnam-do and Gimhae.

Declarations

Conflict of Interest The authors have no conflicts of interest to declare.

References

1. T. Karasawa, and Y. Miyata, *Thin Solid Films* 223, 135 (1993).
2. G.D. Zhou, S.K. Duan, P. Li, B. Sun, B. Wu, Y.Q. Yao, X.D. Yang, J.J. Han, J.G. Wu, G. Wang, L.P. Liao, C.Y. Lin, W. Hu, C.Y. Xu, D.B. Liu, T. Chen, L.J. Chen, A.K. Zhuo, and Q.L. Song, *Adv. Electron. Mater.* 4, 1700567 (2018).
3. G.D. Zhou, Z.J. Ren, B. Sun, J.G. Wu, Z. Zou, S.H. Zheng, L.D. Wang, S.K. Duan, and Q.L. Song, *Nano Energy* 68, 104386 (2020).
4. Y. Galagan, J.E.J.M. Rubingh, R. Andriessen, C.C. Fan, P.W.M. Blom, S.C. Veenstra, and J.M. Kroon, *Sol. Energy Mater Sol. Cells* 95, 1339 (2011).
5. M. Bansal, R. Srivastava, C. Lal, M.N. Kamalasanan, and L.S. Tanwar, *Nanoscale* 1, 317 (2009).
6. Z.C. Wu, Z.H. Chen, X. Du, J.M. Logan, J. Sippel, M. Nikolou, K. Kamaras, J.R. Reynolds, D.B. Tanner, A.F. Hebard, and A.G. Rinzler, *Science* 305, 1273 (2004).
7. D.H. Zhang, K. Ryu, X.L. Liu, E. Polikarpov, J. Ly, M.E. Tompson, and C.W. Zhou, *Nano Lett.* 6, 1880 (2006).
8. H. Kim, C.M. Gilmore, J.S. Horwitz, A. Piqué, H. Murata, G.P. Kushto, R. Schlaf, Z.H. Kafafi, and D.B. Chrisey, *Appl. Phys. Lett.* 76, 259 (2000).
9. T. Stubhan, I. Litzov, N. Li, M. Salinas, M. Steidl, G. Sauer, K. Forberich, G.J. Matt, M. Halikand, and C.J. Brabec, *J. Mater. Chem. A* 1, 6004 (2013).
10. F.L. Wang, N.K. Subbaiyan, Q. Wang, C. Rochford, G.W. Xu, R.T. Lu, A. Elliot, F. D'Souza, R.Q. Hui, and J. Wu, *ACS Appl. Mater. Interfaces* 4, 1565 (2012).
11. K.C. Sanal, M. Majeesh, and M.K. Jayaraj, *Proc SPIE* 8818, 14 (2013).
12. D.Z. Chen, G. Fan, H.X. Zhang, L. Zhou, W.D. Zhu, H. Xi, H. Dong, S.Z. Pang, X.N. He, Z.H. Lin, J.C. Zhang, C.F. Zhang, and Y. Hao, *Nanomaterials* 9, 932 (2019).
13. M.G. Kang, H.J. Park, S.H. Ahn, and L.J. Guo, *Sol. Energy Mater Sol. Cells* 94, 1179 (2010).
14. Y.S. Woo, *Micromachines* 10, 13 (2018).
15. X. Wang, L.J. Zhi, and K. Müllen, *Nano Lett.* 8, 323 (2008).
16. T.M. Higgins, and J.N. Coleman, *ACS Appl. Mater. Interfaces* 7, 16495 (2015).
17. A.K. Sahoo, C.S. Yang, C.L. Yen, H.C. Lin, Y.J. Wang, Y.H. Lin, O. Wada, and C.L. Pan, *Appl. Sci.* 9, 761 (2019).
18. S.P. Rwei, Y.H. Lee, J.W. Shiu, R. Sasikumar, and U.T. Shyr, *Polymers* 11, 134 (2019).
19. L.Q. Yang, T. Zhang, H.X. Zhuo, S.C. Price, B.J. Wiley, and W. You, *ACS Appl. Mater. Interfaces* 3, 4075 (2011).
20. L.B. Hu, H.S. Kim, J.Y. Lee, P. Peumans, and Y. Cui, *ACS Nano* 4, 2955 (2010).
21. C.H. Liu, and X. Yu, *Nanoscale Res. Lett.* 6, 75 (2011).
22. R.Y. Zhang, and M. Engholm, *Nanomaterials* 8, 628 (2018).
23. M. Singh, and S. Rana, *Mater. Today Commun.* 24, 101317 (2020).
24. Y.G. Jia, C. Chen, D. Jia, S.X. Li, S.L. Ji, and C.H. Ye, *ACS Appl. Mater. Interfaces* 8, 9865 (2016).
25. W.X. Zhang, W. Song, J.M. Huang, L.K. Huang, T.T. Yan, J.F. Ge, R.X. Peng, and Z.Y. Ge, *J. Mater. Chem. A* 7, 22021 (2019).

26. S.Y. Lee, J.S. Lee, J.S. Jang, K.H. Hong, D.K. Lee, S.M. Song, K.H. Kim, Y.J. Eo, J.H. Yun, J.H. Gwak, and C.H. Chung, *Nano Energy* 53, 675 (2018).
27. S. Coskun, E.S. Ates, and H.E. Unalan, *Nanotechnology* 24, 125202 (2013).
28. J.L. Elechiguerra, L. Larios-Lopez, C. Liu, D. Garcia-Gutierrez, A. Camacho-Bragado, and M.J. Yacaman, *Chem. Mater.* 17, 6042 (2005).
29. H.H. Khaligh, and I.A. Goldthorpe, *Nanoscale Res. Lett.* 8, 235 (2013).
30. H. Dong, Z.X. Wu, Y.Q. Jiang, W.H. Liu, X. Li, B. Jiao, W. Abbas, and X. Hou, *ACS Appl. Mater. Interfaces* 8, 31212 (2016).
31. F. Duan, W.W. Li, G.R. Wang, C.X. Weng, H. Jin, H. Zhang, and Z. Zhang, *Nano Res.* 12, 1571 (2019).
32. Q.J. Xu, T. Song, W. Cui, Y.Q. Liu, W.D. Xu, S.T. Lee, and B.Q. Sun, *ACS Appl. Mater. Interfaces* 7, 3272 (2015).
33. A.R. Kim, Y.L. Won, K.H. Woo, C.H. Kim, and J.H. Moon, *ACS Nano* 7, 1081 (2013).
34. Y.W. Hu, C. Liang, X.Y. Sun, J.F. Zheng, J.A. Duan, and X.Y. Zhuang, *Nanomaterials* 9, 673 (2019).
35. Y.M. Kim, and J.-W. Kim, *Appl. Surf. Sci.* 363, 1 (2016).
36. C.-H. Hong, S.K. Oh, T.K. Kim, Y.-J. Cha, J. Kwak, J.-H. Shin, B.-K. Ju, and W.-S. Cheong, *Sci. Rep.* 5, 17716 (2015).
37. S.J. Choi, S.I. Han, D.J. Jung, H.J. Hwang, C.H. Lim, S.C. Bae, O.K. Park, C.M. Tschabrunn, M.C. Lee, S.Y. Bae, J.W. Yu, J.H. Ryu, S.-W. Lee, K.P. Park, P.M. Kang, W.B. Lee, R. Nezafat, T.H. Hyeon, and D.-H. Kim, *Nat. Nanotech.* 13, 1048 (2018).
38. G.S. Liu, Y.W. Xu, Y.F. Kong, L. Wang, J. Wang, X. Xie, Y.H. Luo, and B.R. Yang, *ACS Appl. Mater. Interfaces* 10, 37699 (2018).
39. G. Žerjav, and I. Milošev, *Corros. Sci.* 98, 180 (2015).
40. W.J. Yang, T.Q. Li, H.H. Zhou, Z. Huang, C.P. Fu, L. Chen, M.B. Li, and Y.F. Kuang, *Electrochim. Acta* 220, 245 (2016).
41. M. Finsgar, *Spectrochim. Acta Part A Mol. Biomol. Spectrosc.* 190, 290 (2018).
42. J. Lee, P. Lee, H.M. Lee, D.J. Lee, S.S. Lee, and S.H. Ko, *Nanoscale* 4, 6408 (2012).
43. H. Oh, J. Lee, and M. Lee, *Appl. Surf. Sci.* 427, 65 (2018).
44. Y. Qin, S.-M. Lee, A. Pan, U. Gösele, and M. Knez, *Nano Lett.* 8, 114 (2008).
45. S. Xu, P.F. Li, and Y. Lu, *Nano Res.* 11, 625 (2018).
46. X.F. Pan, H.L. Gao, Y. Su, Y.D. Wu, X.Y. Wang, J.Z. Xue, T. He, Y. Lu, J.W. Liu, and S.H. Yu, *Nano Res.* 11, 410 (2018).
47. I. Fratoddi, R. Matassa, L. Fontana, I. Venditti, G. Familiari, C. Battocchio, E. Magnano, S. Nappini, G. Leahu, A. Belardini, R.L. Voti, and C. Sibilia, *The J. Phys. Chem. C* 121, 18110 (2017).
48. L. Zhang, C. Wang, and Y. Zhang, *Appl. Surf. Sci.* 258, 5312 (2012).
49. S. Akel, R. Dillert, N.O. Balayeva, R. Boughaled, J. Koch, M. El. Azzouzi, and D.W. Bahnemann, *Catalysts* 8, 647 (2018).
50. B.A. Zaccheo, and R.M. Crooks, *Langmuir* 27, 11591 (2011).